Journal of Nuclear Energy Science & Power Generation Technology.

Research Article A SCITECHNOL JOURNAL

Design and Analysis of Savonius Vertical Wind Turbine Using Blade Geometry and Flow Augmentation Device

Kannan K* and Jaganath Suriya S

Department of Mechanical Engineering, PSG College of Technology, Coimbatore, Tamil Nadu, India

***Corresponding author:** Kannan K, Professor, Department of Mechanical Engineering, PSG College of Technology, Coimbatore, Tamil Nadu, India, E-mail: 1nkk.mech@psgtech.ac.in

Received date: October 20, 2021; **Accepted date: November** 04, 2021; **Published date: November** 11, 2021

Abstract

Efficiently designed low speed wind turbines can effectively tap the low-grade green energy and thus is an endowment to the society. Owing to the present energy crises (global warming), the researchers around the world are seeking renewable energy sources with low CO2 emission. A Savonius turbine can be operated in any direction, it is simple to construct and the operating speed is less. Inspire of all these features the efficiency is very low additionally it suffers from high negative torque. The aim of the paper is to find the optimal combination of blade geometry and flow augmentation device that improves the efficiency of the turbine and reduces the negative torque. Then the performance of the wind turbine is visualized by CFD simulation because it saves money and experimental efforts compared with the old techniques in wind turbine design. 9 trial combinations of blade geometry are designed and numerical results are obtained using CFD Analysis. Out of 9 trials the combination AR-0.5, OR-0.2 and HA-12.5 turbine gives the maximum torque generation by value of 1.7520 N-m which has a Cp value of 0.31. Further the combination case is modified for design enhancement study with the help of guide vanes which leads to an improvement of torque of 1.9487 N-m and Cp of 0.34.

Keywords: Low wind speed; Savonius vertical axis wind turbine; Torque; Power coefficient; Computational fluid dynamics

Introduction

Wind turbines are usually classified according to its axis of rotation as

(i) Horizontal Axis Wind Turbine (HAWT)

(ii) Vertical Axis Wind Turbine (VAWT)

Savonius turbine was developed and patented by SJ Savonius, is a vertical axis wind turbine that can operate at low wind speed in any direction. The maximum efficiency is 37%. The major drawback of # turbine is its low efficiency which can be improved by changing its design parameters. Recent experimental and numerical studies suggests that, the power coefficient can be improved to the range up to 0.1 and 0.25.

Working Principle

The Savonius wind turbine is a simple vertical axis device having a shape of half-cylindrical parts attached to the opposite sides of a vertical shaft (for two-bladed arrangement) and operate on the drag force, so it can't rotate faster than the wind speed. This means that the tip speed ratio is equal to 1 or smaller. As the wind blows into the structure and comes into contact with the opposite faced surfaces (one convex and other concave), two different forces (drag and lift) are exerted on those two surfaces. The basic principle is based on the difference of the drag force between the convex and the concave parts of the rotor blades when they rotate around a vertical shaft. Thus, drag force is the main driving force of the Savonius rotor. Figure 1-9 shows characteristic parameters of a Savonius wind turbine with two semicircular profile blades.

Butaud and Besnard have highlighted the concept of drag wind turbine for Savonius turbine. The dynamic analysis of its operation shows the influence of lift force. The Savonius can't really be classified into one or the other of these categories. Its efficiency at starting is in fact mainly due to drag force, but its maintenance in rotation is mainly due to the force of lift.

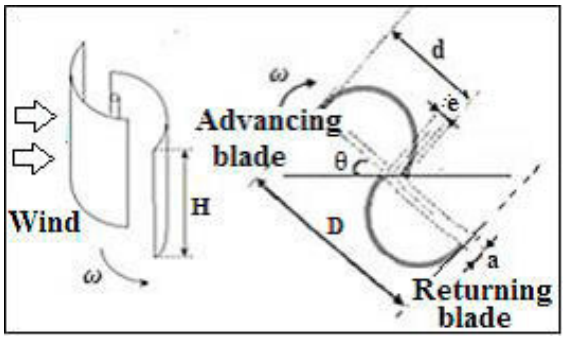

Figure 1: Two-bladed Savonius rotor.

A Review of Literature

There are a few relevant researches in attempting to improve performances of VAWTs at low speed conditions. Takao M et al., developed an air flow controlling device called a "directed guide vane row". This straight-bladed mechanism is inherently constrained due to the design; it can capture a wind stream only in a single direction of a VAWT. Chong, WT et al., developed omnidirectional guide vanes, which can greatly increase power output of a VAWT. Also, Pope K et al., introduced numerical analysis to determine operating angles of stator vanes for a VAWT. Although those devices can capture wind in all directions, proper arrangements of guide vanes are not concerned for best practice in those studies. Additionally, Ohya Y and Karasudani T developed a shrouded horizontal axis wind turbine system called "wind-lens turbine". It can be learnt that wind can be speeded up by a shaped passage even though the design is not applicable to VAWTs. In this study, a wind booster is developed in order to improve angular speed of the VAWT which leads to increase in mechanical power generated from the VAWT. By using specially-designed guide vanes, the wind booster can control flow direction and accelerate wind from any directions in order to yield effective impacts to VAWT blades [1-9].

Parameters that Affect the Performance of Savonius Wind Turbine

Effect of blades number

Rotor's performance is directly affected by number of blades, For 1,2 and 3 stage rotors, optimum blade number is two [10]. A comparison of power coefficient for two and three blades is done by Ali [11] who also concluded that two number of blade is effective.

Effect of aspect ratio

Aspect Ratio (AR) influences the aerodynamic performance of Savonius rotor. The increase of power coefficient with increase in aspect ratio (α - 0.5,1,2,4,5) while keeping other parameters constant was demonstrated by N H Mahmoud [12]. Consistent results of Cp were reported corresponding to the low aspect ratio. Take for example, the maximum Cp was 0.21 when aspect ratio is 0.7 Kamojia et al. [13] and when AR is 0.77, the Cp is 0.24 Modi et al. [14]. However good performance were seen when AR [15] is within the range of 1.5-2.

Effect of overlap ratio

The structure of flow inside the rotor is influenced by overlap ratio which in turn affects the aerodynamic performance. From the literature it was found that the effect of overlap ratio was studied widely. But there was no common accord attained in the results so far.

The optimal value for overlap ratio is 0.1 to 0.15 as per Blackwell et al. [16]. Whereas J Menet et al. [17] showed that the optimal value is 0.242 when the overlap ratio is 0.15 and 0.3. A detailed investigation on overlap ratio was done by Akwa et al. [18] and concluded that the power coefficient is 0.3161 and TSR is 1.25 when overlap ratio is equal to 0.15.

Methodology

The first step in the design process is to validate the base model numerically with that of experimental results to find the suitable turbulence model and algorithm used to solve this turbo machinery problem. After validation 9 different combination models are designed and simulation is performed using ansys fluent. The best combination out of these 9 have been taken for design enhancement study using guide vanes. Finally the results of all 10 different geometries are compared with the base case taken and the suitable combination is found in [19].

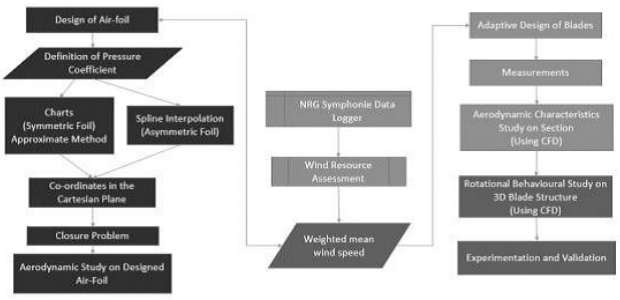

Figure 2: Methodology of the project.

Geometric Modelling of Trial Combinations

The geometric modelling of all the trial combinations is done by solid works software. The diagrammatic representation of trial combinations along with the specifications are mentioned below.

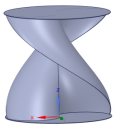

Figure 3: AR-1, OR-0.2, HA-15.

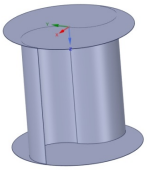

Figure 4: AR-1, OR-0, HA-0.

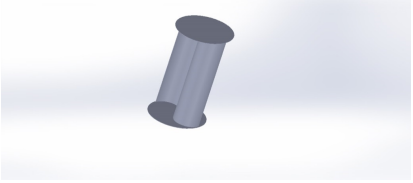

Figure 5: AR-0.5, OR-0, HA-0.

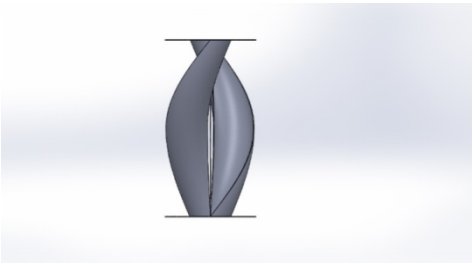

Figure 6: AR-1, OR-0.15, HA-12.5.

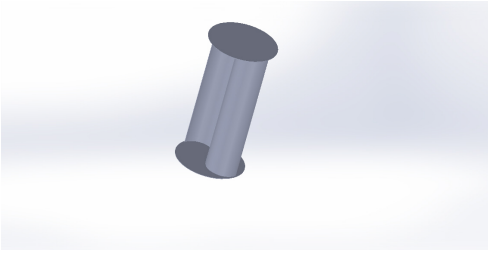

Figure 7: AR-2, OR-0, HA-0.

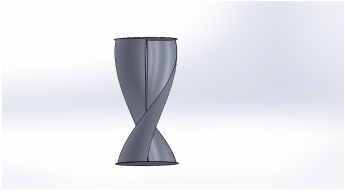

Figure 8: AR-0.5, OR-0.2, HA-12.5.

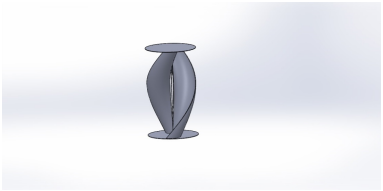

Figure 9: AR-2, OR-0.2, HA-12.5.

Numerical Simulation of Combination Models

Meshing and refinement

Commercial software ansys icem cfd 19.2 has been used to generate an unstructured tetrahedral volume mesh for Fluent. Fine refinements like curvature-proximity capture and improved orthogonal quality of mesh system is carried out. The mesh element size is set at 0.05 m, which effectively works with the system after fair experience. The number of nodes and elements in the geometry are 54840 and 0.279 M and 218420 cells in Figure 10.

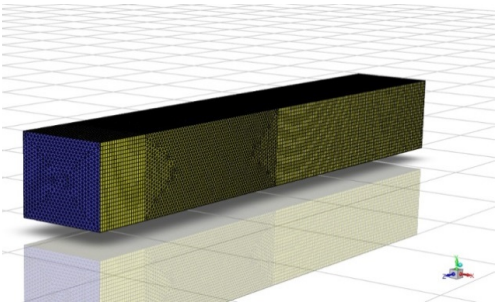

Figure 10: Tetrahedral meshing of wind tunnel.

Conservation equations

The model is set to solve for a pressure-based solver-being an in-compressible flow with density changes less than 5% or Ma<0.3. A transient state simulation is executed to account for writing up of the motion history as set of co-ordinates in variant time steps. The turbulence around the turbine blades can be effectively captured by k - ε model because of its robust nature. Realizable model is preferred for boundary layers under strong adverse pressure gradients, separation and re-circulation. Continuity equation and three dimensional navier stokes equations defines the velocity and pressure at progressive time steps in every nodal point. Non-dimensionalized form of k-ε equations are shown here that are associated with the turbulence model [20-22].

Boundary conditions

A uniform velocity profile is considered at the inlet. Constant magnitude and normal to the boundary-flow condition is imposed at the inlet of 9 m/s in pressure outlet has been applied at the outlet.

Numerical procedure

Finite volume based Solver is used in simultaneous solving of conservation equations in ANSYS Fluent. Pressure and velocity coupling are achieved using Semi-Implicit Method for Pressure Linked Equations (SIMPLE) algorithm. QUICK discretization is used as it provides better accuracy than first order scheme for rotating flows as is the case. Flow courant number remains below 1.0 for all computations. The convergence criteria are set at 10-3 for pressure and momentum convergence.

Moving reference frame

A Moving Reference Frame (MRF) is a relatively simple, robust, and efficient steady-state, Computational Fluid Dynamics (CFD) modeling technique to simulate rotating machinery. For example, the rotors on a quad copter can be modeled with MRFs. **MRF CFD simulation of a quad copter in flight** shows streamlines colored by velocity magnitude

An MRF assumes that an assigned volume has a constant speed of rotation and the non-wall boundaries are surfaces of revolution (e.g., cylindrical, spherical, conical). In the case of the quad copter example the volumes between the rotor blades are designated as MRFs, assigned rotational speeds, and embedded within a multi-volume flow domain. MRF is equivalent to running a rotational simulation and then observing the results at the instant equivalent to the position of the rotor within the MRF. MRF assumes a weak interaction between the MRF volume and the surrounding stationary volumes [23-26].

However, in practice the moving mesh technique often has robustness problems due its dependence on intersection calculations between the stationary and rotating volumes. Also the moving mesh technique is a transient (unsteady) simulation procedure which typically results in extremely long runtimes. Given the significant drawbacks of the moving mesh technique, the MRF is the preferred approach within its limitation in Figure 11-13.

Results of Numerical Simulation

Torque obtained for different wind speeds

The Torque is calculated for three different wind speeds namely 5 m/s, 9 m/s and 13 m/s in Table 1.

Model Description	5 m/s	9 m/s	13 m/s
A	0.4552	1.2161	4.3068
B	0.2066	0.7384	2.2513
C	0.3216	0.9874	3.1562

D	0.3481	0.9914	3.3482
E	0.0124	0.0987	0.1815
F	0.515	1.752	5.0153
G	0.1113	0.377	0.895
H	0.5031	1.5476	4.771
I	0.1085	0.365	0.8895
J	1.255	1.958	7.9839

Table 1: Torque calculation of different wind speeds.

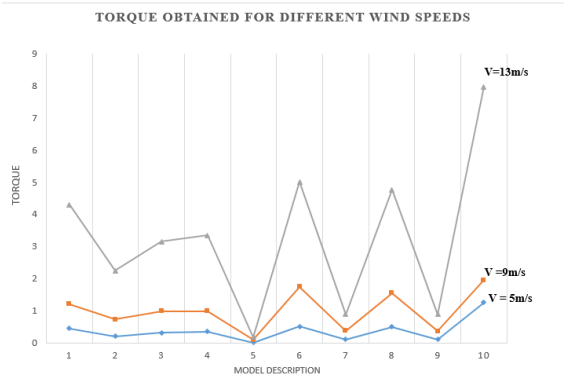

Figure 11: Graphical Representation of Torque obtained for wind speeds 5 m/s, 9 m/s and 13 m/s.

Coefficient of drag for different wind speeds

The Drag Coefficients are calculated for three different wind speeds namely 5 m/s, 9 m/s and 13 m/s in Table 2.

Model description	5 m/s	9 m/s	13 m/s
A	0.18017	0.602	0.9735
B	0.1052	0.319	0.7131
C	0.1532	0.5084	0.7364
D	0.1716	0.5472	0.8851
E	0.0978	0.239	0.3276
F	0.2465	0.7024	2.142
G	0.103	0.318	0.7127
H	0.239	0.7138	1.5567
I	0.1002	0.2812	0.471
J	0.5337	0.7179	3.123

Table 2: Drag coefficient calculation of different winds speeds.

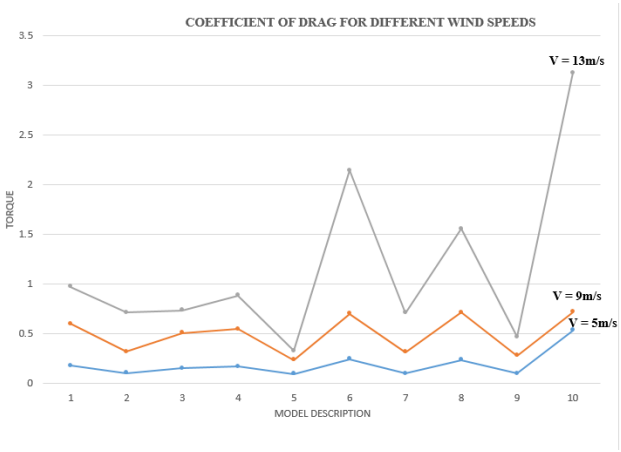

Figure 12: Graphical Representation of Cd obtained for wind speeds 5 m/s, 9 m/s and 13 m/s.

Significance of Helical Angle

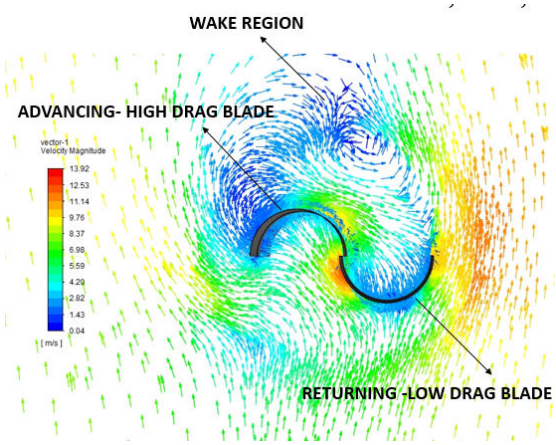

Figure 13: Velocity vector plot.

For AR-2, OR-0, HA-0 combination when the blade profile is a straight and has zero helical angle, the entering fluid impinges both the concave and convex shaped blades. This orientation of blade drives only partial fluid is guided to the advancing blade (concave shaped) and the remaining is diverted away from both the blades. More over there is a considerable wake region behind the blades and backward dragging of the assembly reduces couple generated by the turbine in Figure 14.

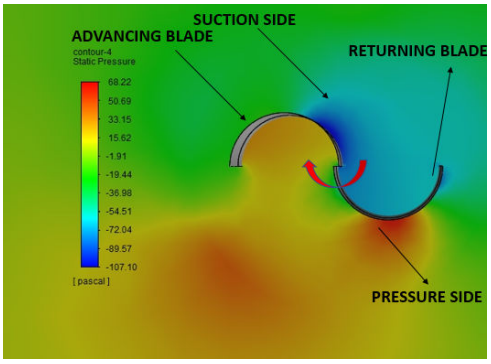

Figure 14: Static Pressure plot.

For AR-2, OR-0, HA-0 combination the returning blade has appropriate pressure side suction side pattern whereas in advancing blade the pattern is adversed. The pressure build up in front of the advancing blade reduces the inflow of upstream air in this region. This physics effectively generates negative torque on the advancing blade and reduces the over all torque. Hence different helical angles are tried to find the best possible angle of twist to make use of wind resource properly in Figure 15.

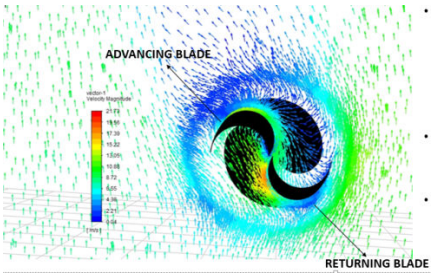

Figure 15: Velocity vector plot.

For AR-0.5, OR-0.2, HA-12.5 combination profile is a helical shaped profile with angle of twist 12.5°. Due to inclination of the blades most of the incoming fluid gets diverted to the advancing blade after striking the convex shaped blade. The directionality of the fluid is also uniform throughout the blade profile. The wake zone is completely invisible in this case which in turn reduces the backward drag and induces more couple/torque in Figure 16.

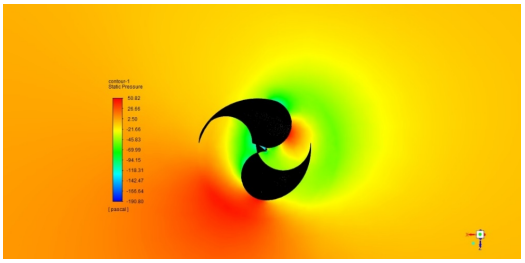

Figure 16: Static Pressure plot.

For AR-0.5, OR-0.2, HA-12.5 combination at this helix angle of 12.5 the pressure/suction are formed in a proper way effectively for both blades and drive the fluid to extract maximum power in Figure 17.

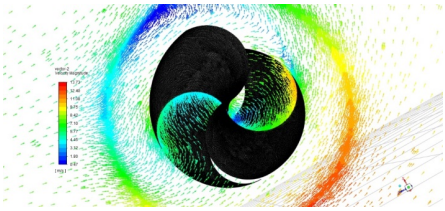

Figure 17: Velocity vector plot.

For AR-1, OR-0.2, HA-15 combination the helical twist of 15°C is working similar to previous case but not as effective as 12.5°C. When compared to straight blade profile this case provides proper direction that guides the fluid through the entire blade profile which will make use of maximum available wind resource and also results in no vortex formation at the rear end of the blades. Still with higher helix angle "stalling" effect is sensed which adverses the performance Figure 18.

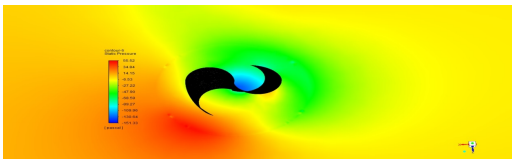

Figure 18: Static Pressure plot.

For helical angle of 15°C the suction and pressure side of the rotor blades are generating enough torque compared to null helical angle case but not as effective as 12.5°C The twist angle beyond 12.5°C does not generate enough positive pressure on the rear end of both blades which will affect the movement of rotor that guides the flow for the returning blade Thus out of different ha tried in this case 12.5 is found to be optimum in Figure 19.

Significance of aspect ratio

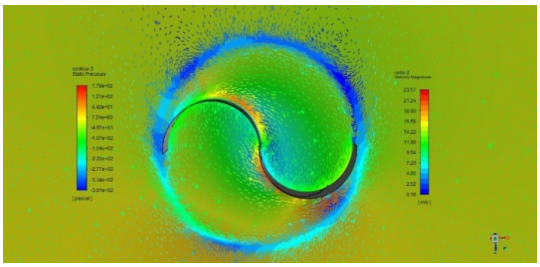

Figure 19: Velocity vector plot.

For AR-0.5, OR-0, HA-0 tssssrial combination the entry of air from pressure side to suction side to neutralize the pressure generates wing tip vortices that significantly reduce the lift or torque. When the diameter of the rotor is smaller, the entry of air from pressure side to suction side take place at a shorter distance from the center of rotation. With the increase in diameter the pressure nullifying takes place only a distance far away from the center of rotation. Thus with the increase in diameter torque increases at the same time too much radial length will arrive at structural instabilities in Figure 20.

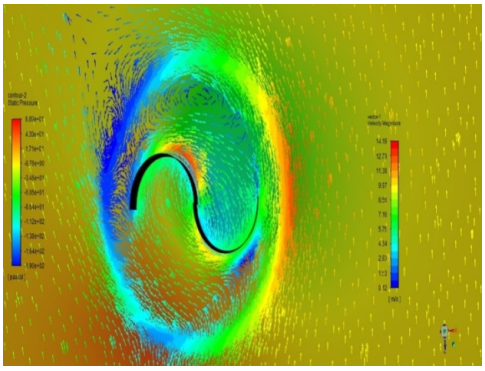

Figure 20: Velocity vector plot.

Wing tip vortices are seen at the tips of the blade with the reduction of radial length of the rotor

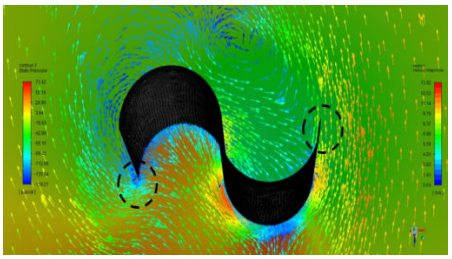

Figure 21: Velocity vector plot.

For AR-2, OR-0, HA-0 high wing tip vortices are visible due to low diameter of the rotor, where the fluid will try to stabilized in pressure. Lesser the diameter more will be chances of formation of wing tip vortices.

Significance of overlap ratio

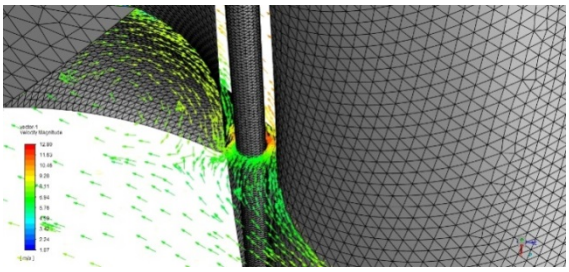

Figure 22: Velocity plots for blade spacing of OR=0.15.

For OR=0.15, overlap ratio explains about the blade spacing provided between the rotor. As the spacing in lower there will be high velocity entering through the spacing that disturbs the wake region at the rear side of turbine which will reduce the momentum of energy extraction [27-29].

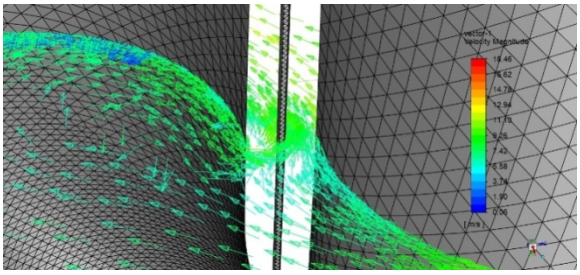

Figure 23: Velocity plots for blade spacing of OR=0.2.

In this case the spacing between the blades will be quite higher compared to the previous case but with increase in spacing the mass flow rate will be higher but the velocity that enters the zone will be less comparing previous one. Significance of overlap ratio is to disturb the wake region and provide positive torque to the rotor in Figure 21-23.

Conclusion

The primary merits of a Savonius rotor are, (i) Simple design (ii) Low starting torque and (iii) Low cost. The only drawback is low efficiency caused by negative torque of the return blade. This paper aims to improve the design of rotor by changing and comparing several combinations of blade geometry and flow augmentation devices and the performance of AR-0.5, OR-0.25, HA-12.5°C with

guide vanes found to be better combination for all the three velocities 5 m/s, 9 m/s and 13 m/s respectively that generates better torque and power compared to existing case. The performance of Savonius can also be improved by adding conveyer or curtain and obstacle shielding. These will increase the complexity of the system, Hence a compromise has to be made between system's simplicity and rotor efficiency which has to be explored more in the future.

References

1. Savonius SJ (1931) The S-rotor and its applications. Mech Eng 53: 333-338.
2. Faruk AA, Sharifian A (2017) Flow field and performance study of vertical axis savonius type SST wind turbine. Energy Procedia 110: 235-242.
3. Jamati F (2011) Eude numérique d'une éolienne hybride asynchrone pp: 1-91
4. Ambrosio MD (2010) Vertical axis wind turbines: History technology and applications pp: 1-90.
5. Roy S, Saha UK (2013) Review of experimental investigations into the design, performance and optimization of the Savonius rotor. PI Mech Eng AJ Pow Energy 227: 528-543.
6. Martin J (1997) Engineer from the national school of arts and crafts B1360 pp: 1-21.
7. Butaud P, Besnard A, Marcel T, Maya M (2013) Unsteady aerodynamic study of a Savonius wind turbine rotor: Demonstration of the influence of lift 21eme Congrès Français de mécanique.
8. Sharma KK, Gupta R, Biswas A (2014) Performance measurement of a two-stage two-bladed Savonius rotor. Int J Renew Energy Res 4: 1-7.
9. Le Gourières D, Énergie éolienne, Eyrolles, Paris,1980.
10. Saha UK, Thotla S, Maity D (2008) Optimum design configuration of Savonius rotor through wind tunnel experiments. J Wind Eng Ind Aerodyn 96: 1359-1375.
11. Ali MH (2013) Experimental comparison study for savonius wind turbine of two and three blades at low wind speed. Int J Mod Eng 3: 2978-2986.
12. Mahmoud NH, Haroun AAEl, Wahba E, Nasef MH (2012) An experimental study on improvement of Savonius rotor performance. Alex Eng J 51: 19-25.
13. Kamojia MA, Kedare SB, Prabhu SV (2009) Experimental investigations on single stage modified Savonius rotor. Appl Energy 86: 1064-1073.
14. Modi VJ, Roth N Fernando MSUK (1984) Optimum configuration studies and prototype design of a wind energy operated irrigation system. J Wind Eng Ind Aerodyn 16: 85-96.
15. Pudur R, Gao S (2015) Performance analysis of Savonius rotor on different aspect ratio for hydropower generation. Conference on power, dielectric and energy management at NERIST. (ICPDEN) pp: 1-6
16. Blackwell BF, Sheldahl RE, Feltz LV (1977) Wind tunnel performance data for two- and three-bucket Savonius rotors. 2: 160-164.
17. Menet JL, Bourabaa N (2004) Increase in the savonius rotors efficiency via a parametric investigation.
18. Akwa JV, Júnior GADS, Petry AS (2012) Discussion on the verification of the overlap ratio influence on performance coefficients of a Savonius wind rotor using computationalfluid dynamics. Renew Energy 38: 141-149.
19. Mohamed MH, Janiga G, Pap E, Thévenin D (2010) Optimization of Savonius turbines using an obstacle shielding the returning blade. Renew Energy 35: 2618-2626.
20. Mohamed MH, Janiga G, Pap E, Thévenin D (2011) Optimal blade shape of a modified Savonius turbine using an obstacle shielding the returning blade. Energy Convers. Manag 52: 236-242.
21. Altan BD, Atılgan M, Özdamar A (2008) An experimental study on improvement of a Savonius rotor performance with curtaining. Exp Therm Fluid Sci 32: 1673-1678.
22. Gad HE, Hamid AAE (2014) A new design of Savonius wind turbine: Numerical study. An International Journal 6: 144-158.
23. Sharma S, Sharma RK (2016) Performance improvement of Savonius rotor using multiple quarter blades a CFD investigation 127: 43-54.
24. Tartuferia M, Alessandro VD, Montelpare S, Ricci R (2015) Enhancement of s avonius wind rotor aerodynamic performance: A computational study of new blade shapes and curtain systems. Energy 79: 371-384.
25. Sanusi A, Soeparman S, Wahyudi S, Yuliati L (2016) Experimental Study of Combined Blade Savonius Wind Turbine. Int J Renew Energy Res 6: 1-6
26. Yao YX, Tang ZP, Wang XW (2013) Design based on a parametric analysis of a drag driven VAWT with a tower cowling. J Wind Eng Ind Aerodyn 116: 32-39.
27. Kailash G, Eldho TI, Prabhu SV (2012) Performance study of modified Savonius water turbine with two deflector plates. Int J Rotating Mach Article ID 679247 pp: 1-12.
28. Ogawa T, Yoshida H (1986) The effects of a deflecting plate and rotor end plates on performance of Savonius type wind turbine. Bulletin of JSME 29: 2115-2121.
29. Iio S, Katayama Y, Uchiyama F, Sato E, Ikeda T (2011) Influence of setting condition on characteristics of Savonius hydraulic turbine with a shield plate. J Therm Sci 20: 224-228.